

ON DETECTION PROBABILITIES OF LINK INVARIANTS

TUOMAS KELOMÄKI, ABEL LACABANNE, DANIEL TUBBENHAUER, PEDRO VAZ AND VICTOR L. ZHANG

ABSTRACT. We prove that the detection rate of n -crossing alternating links by many standard link invariants decays exponentially in n , implying that they detect alternating links with probability zero. This phenomenon applies broadly, in particular to the Jones and HOMFLYPT polynomials and integral Khovanov homology. We also use a big-data approach to analyze knots and provide evidence that, for knots as well, these invariants exhibit the same asymptotic failure of detection.

CONTENTS

1. Introduction	1
2. Proof of the main result	3
3. Big data and categorification	10
References	11

1. INTRODUCTION

Our goal in this paper is to understand the effectiveness of knot invariants (classical, quantum, and beyond) as tools for distinguishing knots. The following theorem captures our main theoretical result.

Theorem 1.1. *All of the marked invariants in Table 1 detect alternating links with probability zero. Even stronger, the detection probability decays exponentially with the crossing number.*

Polynomial	$P(\text{detection}) = 0?$	Homology	$P(\text{detection}) = 0?$
Jones	Yes	Khovanov over \mathbb{Z}	Yes
Alexander	Yes	Odd Khovanov over \mathbb{Z}	Yes
SL_N	Yes	HFK over \mathbb{F}_2	Yes
HOMFLYPT	Yes	Khovanov–Rozansky over \mathbb{Z}	Likely
Jones all colors	Yes	HOMFLYPT over \mathbb{Z} (for knots)	Likely
SL_N for (1^k)	Yes	(1^k) or (k) versions of these	Likely
SL_N for (k)	Yes	Khovanov–Floer theories over \mathbb{F}_2	Likely
SL_N for $(N-1, 1)$	Yes	Other	$P(\text{detection}) = 0?$
HOMFLYPT for (1^k)	Yes	Signature	Yes
HOMFLYPT for (k)	Yes	Determinant	Yes
Kauffman	Yes	Double branched cover	Yes
SO_{2N+1}	Yes	HF of double branched cover	Yes
SP_{2N}	Yes	Algebraic concordance	Yes
SO_{2N}	Yes	Finite type invariants of degree ≤ 10	Yes
G_2	Yes	Many invariants that we forgot to add	Depends, but likely

TABLE 1. Summary of our main results. Green entries (“Yes”) are proved in this paper. Blue entries (“Likely”) indicate invariants for which we outline proof strategies and supply big data evidence, though final arguments remain open.

Classical invariants such as the Alexander polynomial together with the signature, the determinant and others, have long formed the backbone of knot theory. The discovery of the Jones polynomial [Jon85] brought a new era, exposing surprising relations among low-dimensional topology, quantum algebra, and physics, and leading to quantum-group-based invariants such as the Witten–Reshetikhin–Turaev (WRT) invariants [RT91]. Their categorifications, notably Khovanov homology [Kho00] and related developments, recast

2020 *Mathematics Subject Classification.* Primary: 57K16, 62R07, secondary: 57K18, 68P05.

Key words and phrases. Quantum invariants, knot homologies, categorification, big data.

these constructions into homological frameworks with deeper algebraic and geometric content. More recently, additional invariants have entered the picture, further broadening the landscape.

A natural question then arises: *How effective are such invariants (classical, quantum, and beyond) as tools for distinguishing knots?* While viewing invariants purely as classifiers risks obscuring the structural depth and interconnections they reveal, the classification problem is compelling in its own right.

A form of “folk wisdom” (with increasing rigorous and empirical backing, see [[Sto04](#), [DGS25](#), [TZ25](#)] for a very biased sample) suggests:

“Many invariants distinguish a random knot with probability zero.”

That is: Put all knots in a bag, shake, and draw one. How likely is a given invariant (say, the determinant or Khovanov homology) to single it out? For the unknot and Khovanov homology the answer is famously positive [[KM11](#)], but the unknot is exceptional; a generic knot typically shares its invariants with many others.

Our main theoretical contribution makes this intuition precise in a setting we can control: we prove that certain invariants (and plausibly most known ones) fail to distinguish the vast majority of knots. However, the full set of knots is intractable, but miraculously the set of alternating links is not [[Tut63](#), [ST98](#)], so we restrict attention to alternating links, where our main theorem [Theorem 1.1](#) applies. The key tool is oriented mutation: following [[Sto04](#)], we show that the set of alternating links modulo oriented mutation is exponentially smaller, so invariants insensitive to such mutation exhibit exponentially decaying detection probability.

Alternating links and oriented mutation should be viewed as methodological devices rather than the ultimate focus. To probe the situation for knots themselves, we complement the theory with large-scale “big data” computational experiments in the spirit of [[LHS22](#), [DGS24](#), [LTV24](#), [DGS25](#), [TZ25](#)]. These experiments concentrate on quantum invariants, comparing polynomial invariants to their categorifications and measuring detection rates across extensive datasets. Strikingly, the results reveal essentially no performance gap between polynomials and their homological lifts. This approach and its results are arguably more important than the “folk theorem” [Theorem 1.1](#) itself.

1A. Some remarks. Before we prove [Theorem 1.1](#), let us collect some remarks.

Remark 1A.1. Links are easier to study asymptotically than knots, but we do not expect a huge difference between the detection rates. More crucial is the restriction to alternating links (to be precise, we mean non-split alternating links), and we do not know how to adjust our proof to include non-alternating links (see [Remark 2.13](#) for more details). However, we expect the detection rate on non-alternating to be worse than on alternating links, see [Section 3](#) (and [[DGS25](#), [TZ25](#)]) for data-driven evidence. ◇

Remark 1A.2. (Why this phenomenon is not surprising.) There are several reasons to expect that many knot invariants perform poorly as classifier. Recorded below is one concrete reason, while another is the “folk wisdom” mentioned above.

One would expect, say, quantum invariants to perform exceptionally well on knots with few crossings, and indeed they do (cf. [Section 3](#)). In contrast, detection across the entire set of knots is widely expected to be very difficult, even if formal results are limited. As evidence, many nearby decision/optimization problems are already hard: for example, knot genus is NP-hard [[AHT06](#)], and the (graph) crossing number admits no constant-factor approximation unless $P = NP$ [[Cab13](#)]. Such barriers make it unrealistic to expect generic invariants, many of which are “efficiently” computable in practice, to act as effective classifiers at scale. In contrast, strong invariants provide a practical remedy, e.g. the knot complement is a complete invariant of a knot by [[GL89](#)], but the associated 3-manifold decision problems are expected to be very difficult, see, for example, [[AFW15](#)] for a summary. ◇

Remark 1A.3. (Why this phenomenon is surprising.) We had no a priori reason to expect the invariants in [Theorem 1.1](#) to have detection probability zero, so the theorem was genuinely surprising to us (even if there were hints). To emphasize why [Remark 1A.2](#) does not translate into statements about detection probabilities, we give an analogy: deciding whether a graph contains a Hamiltonian cycle is NP-complete, yet in the standard random-graph models the heuristic “Every graph is Hamiltonian” is asymptotically correct with probability one (i.e. asymptotically almost surely).

Equally striking is the rate of decay: in our data, the Jones polynomial detects only about 40% of prime knots with at most 18 crossings; see [Section 3](#). ◇

Acknowledgments. We thank Radmila Sazdanovic, whose talk (York, July 2024) sparked this project. We used ChatGPT to assist with coding, proofreading, conjecture generation, and aspects of proof development, and we gratefully acknowledge this support. We thank Alexis Langlois-Rémillard for pointer to the literature, which sparked part of this collaboration. Part of this project was done while the second author visited the fourth author at the Université catholique de Louvain, and their hospitality is gratefully acknowledged.

This work used the Katana computational cluster (DOI: <https://doi.org/10.26190/669X-A286>), supported by Research Technology Services at UNSW Sydney, and some of the computations were performed using the resources of the Laboratoire de Mathématiques Blaise Pascal.

DT acknowledges support from the ARC Future Fellowship FT230100489 and suspects their role will soon be outsourced to AI.

2. PROOF OF THE MAIN RESULT

We now explain and prove the statement in the title, and even the generalization in [Theorem 1.1](#) of it. But before we start:

Remark 2.1. This paper is largely self-contained; however, we assume the reader has some familiarity with knot theory and analytic combinatorics. For background in these areas, we recommend standard references such as [\[Ada94, FS09\]](#). Beginning after [Theorem 2.18](#), we also rely on several standard tools from the theory of quantum invariants. For background on these, see for example [\[Tur94, Oht02, Tub25\]](#) for the polynomial invariants and [\[BN02, Kho06\]](#) for homological invariants. \diamond

Our proof is a variation of arguments from [\[Tut63, ST98, Sto04\]](#), where the main work was done.

Lemma 2.2. *Fix two sequences of sets X_n, Y_n with $n \in \mathbb{Z}_{\geq 0}$, and let $\alpha, \beta \in \mathbb{R}_{\geq 1}$. Then we have*

$$\left(\limsup_{n \rightarrow \infty} \sqrt[n]{\#Y_n} \leq \alpha < \beta \leq \liminf_{n \rightarrow \infty} \sqrt[n]{\#X_n} \right) \text{ implies } \left(\frac{\#Y_n}{\#X_n} \in O(\gamma^n) \text{ for some } \gamma \in (0, 1) \right).$$

Moreover, γ can be chosen to be $\gamma = \frac{\alpha+\varepsilon}{\beta-\varepsilon}$ for some $\varepsilon > 0$.

The same holds when replacing $\#Y_n$ and $\#X_n$ by $\sum_{k=0}^n \#Y_k$ and $\sum_{k=0}^n \#X_k$ on the right-hand side.

Proof. The result is straightforward and omitted. However, curious readers may consult the proof generated by ChatGPT (model 5), reproduced here with its permission.

Choose $\varepsilon > 0$ with $\alpha + \varepsilon < \beta - \varepsilon$ and set $r_1 := \alpha + \varepsilon$, $r_2 := \beta - \varepsilon$; then $1 < r_1 < r_2$. By the \limsup / \liminf hypotheses, for $n \gg 0$ we have $\#Y_n \leq r_1^n$ and $\#X_n \geq r_2^n$, hence

$$\frac{\#Y_n}{\#X_n} \leq \left(\frac{r_1}{r_2} \right)^n =: \gamma^n, \quad \gamma \in (0, 1).$$

For the summed version, note that

$$\sum_{k=0}^n \#Y_k \leq \sum_{k=0}^n r_1^k = \frac{r_1^{n+1} - 1}{r_1 - 1} \leq \frac{r_1}{r_1 - 1} r_1^n, \quad \sum_{k=0}^n \#X_k \geq \#X_n \geq r_2^n.$$

Therefore

$$\frac{\sum_{k=0}^n \#Y_k}{\sum_{k=0}^n \#X_k} \leq \frac{r_1}{r_1 - 1} \left(\frac{r_1}{r_2} \right)^n = C \gamma^n$$

with the same $\gamma \in (0, 1)$ and a constant $C > 0$ independent of n . \square

Let $(X_n)_{n \in \mathbb{Z}_{\geq 0}}$ be a sequence of nonempty finite sets such that $X_n \subset X_{n+1}$ for all $n \in \mathbb{Z}_{\geq 0}$. Define the limiting set

$$X := \bigcup_{n=0}^{\infty} X_n.$$

Let Y be a subset of X and define, for all $n \in \mathbb{Z}_{\geq 0}$, $Y_n = Y \cap X_n$.

Lemma 2.3. *In the setting of [Lemma 2.2](#), the probability that a random $x \in X$ is in Y is zero (with this notion made precise in the proof and used thereafter).*

Proof. We have that the relative sizes decay exponentially, i.e. for large enough n :

$$\frac{\#Y_n}{\#X_n} \leq C \cdot \gamma^n, \quad \text{for some constants } C \in \mathbb{R}_{>0}, \gamma \in (0, 1).$$

Then Y has asymptotic density zero in X , in the sense that

$$\lim_{n \rightarrow \infty} \frac{\#(Y \cap X_n)}{\#X_n} = \lim_{n \rightarrow \infty} \frac{\#Y_n}{\#X_n} = 0.$$

In particular, if we equip X_n with the uniform probability measure, meaning

$$\mathbb{P}_n(x) = 1/\#X_n, \quad x \in X_n,$$

then the probability that a randomly chosen element of X_n lies in Y_n tends to zero exponentially:

$$\mathbb{P}_n(x \in Y) = \mathbb{P}_n(x \in Y_n) = \frac{\#Y_n}{\#X_n} \leq C \cdot \gamma^n.$$

In probabilistic terms, this means:

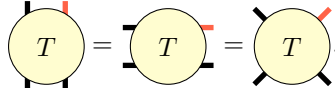
$$\lim_{n \rightarrow \infty} \mathbb{P}_n(x \in Y) = 0.$$

By defining $\mathbb{P}(x \in Y)$ to be $\lim_{n \rightarrow \infty} \mathbb{P}_n(x \in Y)$, this implies the claim, but something even stronger is true: Since $\sum_n \mathbb{P}_n(x \in Y)$ converges (by exponential decay), the Borel–Cantelli lemma gives that

$$\mathbb{P}(x \in Y \text{ infinitely often}) = \limsup_{n \rightarrow \infty} \mathbb{P}_n(x \in Y) = 0,$$

which implies that even countably many randomly chosen $x \in X$ avoid Y . So almost surely a randomly chosen $x \in X$ eventually avoids Y entirely. \square

Below, we will only consider tangles with four boundary points and call them **tangles** for short. We draw them in circles where one boundary string is marked (so that we can number the boundary strings, say clockwise starting from the marked one). Here is an example, the tangle is called T :



The building blocks that we use are

$$0: |, \quad (\infty: \overline{\quad},) \quad 1: \text{X}, \quad -1: \text{X}.$$

The basic operations on such tangles are horizontal and vertical concatenation, called sum, defined as follows. For tangles S and T (where we use dashed lines for the marked strand of S):

$$(2.4) \quad S +_h T = \begin{array}{c} \text{circle with boundary line} \\ \text{marked with red line} \end{array} \quad S +_v T = \begin{array}{c} \text{circle with boundary line} \\ \text{marked with red line} \end{array}$$

Recall that a **rational tangle** is a tangle obtained by (horizontally or vertically) adding the tangles ± 1 to the tangle 0. Such a tangle is **prime** if it cannot be composed into two different nontrivial (neither 0 nor ∞) summands using (2.4).

Let us use the following notation for rational tangles (illustrated with three crossings; the evident generalization applies):

$$3: \text{X} \text{X} \text{X}, \quad -3: \text{X} \text{X} \text{X}, \quad \bar{3}: \text{X} \text{X} \text{X}, \quad -\bar{3}: \text{X} \text{X} \text{X}.$$

The notion of a rational tangle is often defined geometrically, but we will not need the geometric incarnation. The connection between our definition and the geometric is the following lemma.

Lemma 2.5. *Every rational tangle can be obtained as a finite alternating sequence of the form $a_1 +_h \bar{a}_2 +_v a_3 +_h \bar{a}_4 +_v \dots$ or $\bar{a}_1 +_h a_2 +_v \bar{a}_3 +_h a_4 +_v \dots$ for some $a_i \in \mathbb{Z}$.*

Proof. Well-known (this is essentially Conway's classification of rational tangles), see for example [Ada94, Section 2.3]. \square

Let \mathcal{AL}_n be the set of prime alternating links of $\leq n$ crossings. We will use the second part of Lemma 2.2 above strategically and will not distinguish between the sets of knots with $\leq n$ or $= n$ crossings.

Lemma 2.6. *We have*

$$\liminf_{n \rightarrow \infty} \sqrt[n]{\#\mathcal{AL}_n} = \lim_{n \rightarrow \infty} \sqrt[n]{\#\mathcal{AL}_n} = \frac{\sqrt{21001} + 101}{40} > 6.1479.$$

Proof. The proof is a mild variation of [ST98]. Before proving Lemma 2.6, let us give an example of the proof strategy in a baby case.

Example 2.7. The Fibonacci numbers satisfy the recursion $F_0 = 0$, $F_1 = 1$ and $F_{n+1} = F_n + F_{n-1}$ for $n \geq 1$. Let $F(z) = \sum_{n \geq 0} F_n z^n$ be the generating function. The recursion (essentially immediately) gives the functional equation $(1 - z - z^2)F(z) = z$ with poles at $x = 1/\phi$ and $y = -\phi$, for the golden ratio ϕ . Since x is the smallest pole, classical theory then implies $\lim_{n \rightarrow \infty} \sqrt[n]{F_n} = x^{-1} = \phi$. Summarized:

recursion \Rightarrow functional equation \Rightarrow smallest singularity \Rightarrow growth rate.

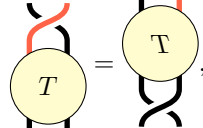
(Here and in what follows, smallest for singularities is meant in terms of absolute value.) We apply the same strategy throughout. \diamond

With [Example 2.7](#) in mind, the proof can be summarized as:

planar algebra/operad \Rightarrow recursion \Rightarrow functional equation \Rightarrow smallest singularity \Rightarrow growth rate.

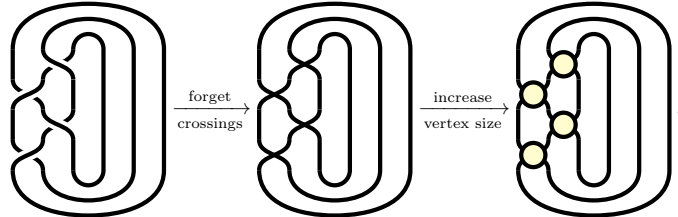
To get started, recall from e.g. [\[ST98\]](#) that:

- (a) Taking the n -th root, there is no difference between the growth rate of prime alternating links and prime alternating tangles.
- (b) Any two alternating link or tangle diagrams are related by a finite number of operations of the form

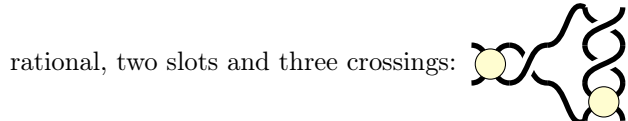


and all variations of this picture. These operations are often called *flypes*.

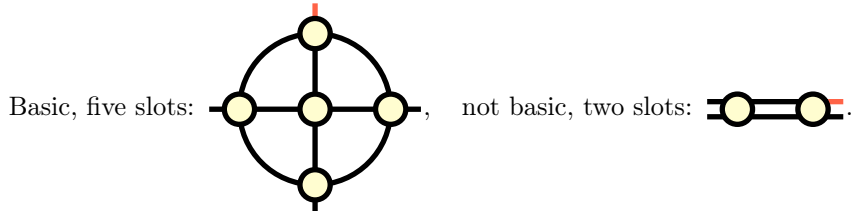
For the proof, recall the *cookie-cutter* operation. This operation takes a link diagram and produces a four-valent planar graph with crossings by replacing some crossings with a vertex, e.g.:



The result is often called a *template* and the cookie-cutter has produced *slots*, and the same procedure (under the same name) applies to tangles. For both, templates and tangles, we can and will use the sum operation in [\(2.4\)](#) for them as well. Moreover, a template is called *rational* if it comes from a rational tangle. The trivial template is the rational template obtained by cookie-cutting the crossing of the tangle 1. Here is an example of a rational template:



Note that a template can still have crossings. A (tangle) template is *basic* if it has no crossings, more than one slot, is prime in the sense of the operation [\(2.4\)](#), and any circle meeting the template in four points encloses either the whole template or a single slot. Here is an example and a nonexample:



Let bt_n be the number of basic templates with n slots. The following is Tutte's miracle.

Lemma 2.8. *The generating function for bt_n is*

$$bt(z) = \frac{(1-4z)^{3/2}(z+1) - 2z^5 - 10z^4 - 10z^3 + 5z - 1}{2(z+1)(z+2)^3}.$$

The smallest singularity is at $z = 1/4$.

Proof. The key trick is to see that basic templates and so-called rooted c-nets are the same, and the latter have been counted in [\[Tut63\]](#). From the formula for $bt(z)$ it is then straightforward to see that the singularities are at $z = 1/4$, $z = -1$, and $z = -2$. \square

Now, the recursion:

Lemma 2.9. *Any tangle diagram can be uniquely constructed by repeatedly inserting templates into designated slots, ensuring that any template inserted into a rational template is a basic template.*

Proof. This works as follows. Call a circle that meets the tangle in four points maximal if it does not enclose the whole tangle or a single crossing, and does not enclose a nontrivial sum of tangles under the operation (2.4). Take the interiors of maximal circles in a tangle diagram, and these tangle diagrams are associated with basic templates, by construction, which can be again obtained by cutting along maximal cycles. \square

Lemma 2.10. *Every ftype that can occur in a tangle diagram can be traced back to a ftype of a rational template somewhere in the hierarchy described in Lemma 2.9 above.*

Proof. Exercise. \square

Lemma 2.10 and (b) above taken together mean that once we have identified all distinct ftype-equivalence classes of rational templates, we can ignore ftypes entirely.

Let $at(z)$ be the generating function of the number of alternating prime tangles. Taking all these observations together gives the functional equation

$$(2.11) \quad at(z) = rt(bt(at(z)), z),$$

where $rt(y, z)$ is the generating function of rational templates up to ftype equivalence, z encodes the number of crossings and y the number of slots so that $rt_{m,n}$, the coefficient of $y^m z^n$, is the number of them with m slots and n crossings. Since $bt(z)$ was identified in [Lemma 2.8](#), it remains to get a handle on $rt(y, z)$.

Lemma 2.12. *The generating function for $rt_{m,n}$ satisfies*

$$2rt(y, z) = 1 + z - y - \left((1 - z + y)^2 - \frac{8(z^2 - yz + y)}{1 - z} \right)^{1/2}.$$

Proof. A bit longish, but nicely explained in [\[ST98\]](#). \square

One can now use [Lemma 2.8](#), [Lemma 2.12](#) and (2.11), and get the equation

$$\frac{135z^2 + 101z - 20}{108(z - 1)} = 0 \Rightarrow 135z^2 + 101z - 20 = 0,$$

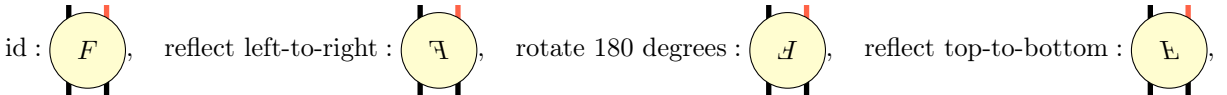
for the singularities of $at(z)$. The statement follows by (a). This finishes the proof of [Lemma 2.6](#). \square

Remark 2.13. (*Why the restriction to alternating links.*) Note that the proof of [Lemma 2.6](#) crucially uses the strategy of [Example 2.7](#), but also that we understand the difference between alternating link diagrams and alternating links with n crossings. This is not true for link diagrams and links (the number links for a given crossing number is usually an order of magnitude smaller than the number of link diagrams) which is why the above strategy would only give a lim sup instead of a lim. Having a statement about lim sup is enough for the next count in [Lemma 2.15](#) only because we have an honest lim in [Lemma 2.6](#).

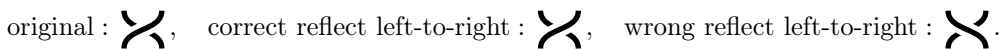
Similarly, Tutte's miracle [Lemma 2.8](#) cannot be used to count alternating knots (the number of components is invisible for basic templates), and we do not know any analog of [Lemma 2.6](#) for knots. The closest result we know is [\[Cha18, Theorem 5\]](#), which however is not strong enough for our count.

These are the main reasons to restrict to alternating links. \diamond

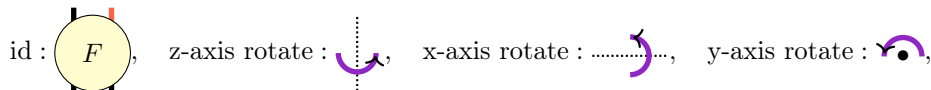
Conway mutation along a tangle, **mutation** for short, is the operation of cookie-cutting a tangle from a link, perform any of the four operation in the symmetry group of the square given by (here displayed using the letter F because its very asymmetric)



where we think of the last operation as a composition of the other nontrivial operations, and then reinsert the manipulated tangle. Here the reflect left-to-right is done in a way that the crossings need to be mirrored:



A better, but three-dimensional, way of saying this is (in the same order as above):



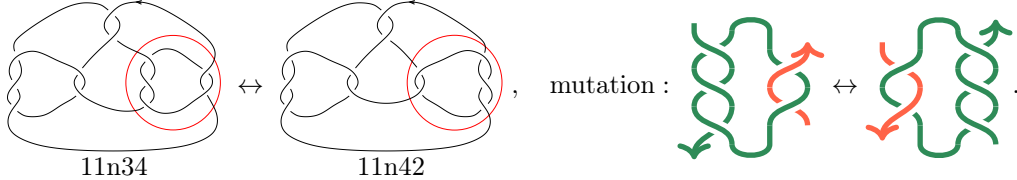
with standard coordinate system. All of these are **mutants** of the original.

Oriented mutation (also called *positive mutation*) is defined in the same way, but without the restriction that the tangles for the mutation have to admit the same orientation before and after mutation. For knots, this cuts the number of mutants in half as only two of the four mutants will allow an induced orientation.

Example 2.14. A good example of oriented mutation to keep in mind is the following:

$$\text{original : } \uparrow \uparrow \downarrow \uparrow, \text{ reflect left-to-right : } \downarrow \uparrow \uparrow \uparrow.$$

Another example, the famous pair of the Kinoshita–Terasaka (11n_42) and the Conway knot (11n_34) is an example of oriented mutation; here are the corresponding pictures from KnotScape:



Here the left-hand sides of the knot diagrams are the same, and we mutate along $\bar{3} +_h \bar{2}$ as on the right. \diamond

Let \mathcal{ALOM}_n be the set of alternating links of n crossings modulo oriented mutation.

Lemma 2.15. *We have*

$$\limsup_{n \rightarrow \infty} \sqrt[n]{\#\mathcal{ALOM}_n} \leq \frac{7(15631 + \sqrt{501732121})}{43334} < 6.1433.$$

Proof. The argument is a variation of [Lemma 2.6](#), and to make it work we adapt the strategy of [\[Sto04\]](#). We start with the following lemma.

Lemma 2.16. *Oriented mutation can be used to permute the summands (cf. [Lemma 2.5](#)) of a rational tangle. The same is true for rational templates.*

Proof. The illustration

$$-2 +_h -\bar{3} = \text{tangle} \xrightarrow{\text{reflect left-to-right}} \text{tangle} = -\bar{3} +_h -2,$$

generalizes easily. One can also think of this as rational tangles are determined by a rational number, so this is actually just an isotopy. Now, for our purposes flypes are isotopies, so for rational templates we first use flypes to reorder within $\pm n, \pm \bar{n}$, e.g.:

$$\text{tangle} \xrightarrow[\text{bottom}]{\text{cookie cut}} \text{tangle with circle } T = \text{circle } T \xleftarrow[\text{top}]{\text{cookie cut}} \text{tangle}.$$

Now, in the previous picture if we would have a slot somewhere, say at the extremities by the above argument, we need actual mutation to go from left to right:

$$\text{tangle with slot} \xrightarrow{\text{reflect left-to-right}} \text{tangle with slot}.$$

But this is oriented mutation as the rational tangle type does not change, as we mentioned above. For example,

$$\text{circle } T \text{ works for } \text{tangle} \text{ and } \text{tangle}.$$

Similarly for the other possibility, and larger cookie cuts. \square

By [Lemma 2.16](#) we can now consider rational templates up to permutation of summands in our count of equivalence classes of prime alternating links modulo oriented mutation. In doing so, we overshoot the actual count, but this is irrelevant for the \limsup statement we want to prove.

As in the proof of [Lemma 2.6](#), recall that $rt(y, z)$ denotes the generating function of rational templates up to flype equivalence for which we have [Lemma 2.12](#). Incorporating permutation of summands we get the generating function $rtp(y, z)$ for the respective sequence $rtp_{m,n}$ of upper bounds.

Lemma 2.17. *The generating function (r for short) for $rtp_{m,n}$ satisfies*

$$-2r^2(y-1) + r(y-1)(3y-z+1) - y^3 + y^2(z+1) + y + \frac{z^2}{1-z} = 0.$$

Proof. A bit nasty, but a direct adaptation of [Sto04, Proof of Theorems 1 and 2]. \square

As before, one can now use Lemma 2.8 and Lemma 2.12 and get the equation

$$\frac{145530z^2 + 109417z - 21667}{233280(z-1)} = 0 \Rightarrow 145530z^2 + 109417z - 21667 = 0,$$

for the singularities of the upper bound generating function we are interested in. The claim follows by solving this equation. \square

Given an invariant of links Q , we define

$$Q(n)_{AL}^{\%} = \#\{Q(L) \mid L \in \mathcal{AL}_n\} / \#\mathcal{AL}_n.$$

That is, $Q(n)_{AL}^{\%}$ measures the proportion of distinct values attained by Q on prime alternating links with n crossings. We say that Q is **insensitive to oriented mutation** if $Q(L) = Q(L')$ whenever L and L' are related by a finite sequence of oriented mutations.

Theorem 2.18. (Exponential decay.) *For any link invariant Q that is insensitive under oriented mutation we have*

$$Q(n)_{AL}^{\%} \in O(\delta^n) \text{ for some } \delta = \delta(Q) \in (0, 0.9993).$$

Moreover, Q detects alternating links with probability zero.

Proof. Note that we have

$$6.1433/6.1479 < 0.9993.$$

Now we combine Lemma 2.2, Lemma 2.6 and Lemma 2.15 for $X_n = \mathcal{AL}_n$ and $Y_n = \mathcal{ALOM}_n$ (which can be regarded as a subset of X_n by taking representatives). The final statement follows then from Lemma 2.3. \square

We need two definitions and a lemma, which are essentially borrowed from [TZ25]. We use quantum invariants to mean the same as in that paper (both, polynomial and homological).

(i) A **skein relation** is a relation of the following form. Let a, b, c be elements in a ring, then

$$a \cdot \text{Diagram} + b \cdot \text{Diagram} + c \cdot \text{Diagram} = 0, \quad \text{for } a, b \text{ invertible.}$$

(ii) **Multiplicity freeness** of a quantum invariant is the property that $V \otimes V$ is multiplicity free, where V is the representation used to color the link components.

The following is well-known, but we sketch a proof for completeness.

Lemma 2.19. *Any polynomial quantum invariant that satisfies a skein relation or is multiplicity free is invariant under (general) mutation.*

Proof. Given a skein relation, one can proceed as follows. The key idea is that the associated invariant is constant on skein equivalence classes, where two diagrams are skein equivalent if they are related by a sequence of skein moves and isotopies. One can then show that mutation preserves skein equivalence by induction on the number of crossings in the mutated tangle: smoothing a crossing yields a skein triple whose mutated versions remain skein equivalent, allowing the inductive step to go through.

To show invariance under mutation in the multiplicity-free case, observe that multiplicity-freeness ensures that the endomorphism associated with a 4-point tangle is diagonal (in a suitable basis), and hence commutes with all other such endomorphisms. A Conway mutation acts by stacking or conjugating with crossing-like tangles that preserve the four boundary points. Since conjugation preserves diagonal operators, the induced endomorphism remains unchanged, and thus the invariant is unaffected by mutation. \square

Proof of Theorem 1.1. We first stay with the class of prime alternating links. All of the invariants marked in Table 1 are invariant under oriented mutation:

- ▶ For the polynomial invariants, except SL_N for $(N-1, 1)$ and the exterior and symmetric HOMFLYPT polynomial, this follows from Lemma 2.19. For SL_N for $(N-1, 1)$ this is [MC96, Theorem 6], and for HOMFLYPT this follows from stabilization (e.g. by following the process described in [TVW17, Section 4]).
- ▶ For Khovanov homology over \mathbb{F}_2 or odd Khovanov homology this follows from [Weh10] and [Blo10].
- ▶ The remaining ones this is a classical result, see [Mor15] for a summary, or can be found in [Gre13].

Additionally:

- For integral Khovanov homology, by [Lee05, Theorem 1.4] and [Shu21, Corollary 1.J], it depends only on the Jones polynomial, signature and a combinatorial formula involving linking numbers (as in [Lee05, Proposition 4.3]). All of these are invariant under mutation: seen above for the Jones polynomial and the signature, and for the formula this is [Lemma 2.20](#) below.
- For HFK over \mathbb{F}_2 the same argument works using [MO08, Theorem 2].

Now apply [Theorem 2.18](#).

For composite alternating links (which are uniquely determined by their prime factors) we need multiplicativity or additivity, i.e. the invariant under consideration Q satisfies

$$Q(L \# M) = Q(L)Q(M) \text{ or } Q(L \# M) = Q(L) + Q(M),$$

or some variation of this.

- For the polynomials multiplicativity is implicit in the surgery/TQFT construction, cf. [Tur94].
- For the homological invariants this follows from [Kho02, Put16].
- For the remaining invariants this is classical, but finite-type invariance deserve a few extra words (details are e.g. in [BN95]): These form a filtered Hopf algebra; primitives are additive under connected sum, and a general invariant of degree d is a polynomial in primitives of degrees $\leq d$, which is enough for what we want.

Here is then the final lemma:

Lemma 2.20. *Let L and L' be oriented links related by an oriented mutation. Then the combinatorial expression for $\dim_{\mathbb{Q}} H_{\text{Lee}}^*(L; \mathbb{Q})$ given in [Lee05, Proposition 4.3] takes the same values for L and L' .*

Proof. Let us start by dividing the components of L into three disjoint sets C_{in} , C_{out} and $\{a, b\}$. The set C_{in} contains the components of L which are completely inside the mutation disk, C_{out} those that are outside of the disk, and $\{a, b\}$ has the remaining one or two components. The components of L are identified with the corresponding components of L' with a and b being identified with the respective components of L' which agree with them outside the mutation disk. We denote $\text{lk}_{x,y}$ as the linking number of x and y in L and $\text{lk}'_{x,y}$ as the linking number of the corresponding components in L' .

The combinatorial expression for the rational Lee homology is given by

$$\dim_{\mathbb{Q}} H_{\text{Lee}}^i(L; \mathbb{Q}) = \#\left\{E \subset \{\text{components of } L\} \mid \sum_{x \in E, y \notin E} 2 \text{lk}_{x,y} = i\right\}.$$

To show that this is invariant under oriented mutation, we construct a bijection

$$\varphi: \{E \subset \{\text{components of } L\}\} \rightarrow \{E \subset \{\text{components of } L'\}\}$$

by

$$\varphi(E) = \begin{cases} E & \text{if } a, b \in E \text{ or } a, b \notin E, \\ (E \cap (\{a, b\} \cup C_{\text{out}})) \cup (E^c \cap C_{\text{in}}) & \text{otherwise.} \end{cases}$$

The linking numbers of L and L' either agree, $\text{lk}_{x,y} = \text{lk}'_{x,y}$, or admit a symmetry $\text{lk}_{a,x} = \text{lk}'_{b,x}$ and $\text{lk}_{b,x} = \text{lk}'_{a,x}$ whenever $x \in C_{\text{in}}$. It follows that

$$\sum_{x \in E, y \notin E} \text{lk}_{x,y} = \sum_{x \in \varphi(E), y \notin \varphi(E)} \text{lk}'_{x,y}$$

for all E and thus $\dim_{\mathbb{Q}} H_{\text{Lee}}^i(L; \mathbb{Q}) = \dim_{\mathbb{Q}} H_{\text{Lee}}^i(L'; \mathbb{Q})$. □

The proof is complete. □

If we would have to summarize the above in an informal way, then it would have to be:

$$(2.21) \quad \boxed{\text{Any local relation on the set of knots forces exponential decay.}}$$

However, this is not a statement we can prove, so it should be taken with a pinch of salt. In any case, the TQFT-like fashion in which quantum invariants are defined makes them exciting on the one hand (e.g. for computations, provable statement etc.) but is a fundamental drawback for them being knot invariants on the other hand.

Remark 2.22. With (2.21) in mind, the above strategy should also apply to Khovanov–Rozansky, and HOMFLYPT homology. For Khovanov homology, mutation invariance is delicate; see [Weh03, LC19], but we found a way around this for alternating links; cf. above. For HOMFLYPT homology (and partially for Khovanov–Rozansky homology), [Jae11, Corollary 1.2] establishes insensitivity to oriented mutation in the case of knots. Nevertheless, numerous subtleties remain, some potentially quite difficult, such as restricting results from links to knots (cf. [Remark 2.13](#)), and we therefore chose not to pursue this direction in the present work. ◇

3. BIG DATA AND CATEGORIFICATION

We now closely follow [TZ25], but restrict our attention to detection of knots.

Remark 3.1. All data files and additional material (such as interactive playgrounds, higher resolution pictures, code, a possible empty erratum and much more) can be found online at [KLTZ25]. In addition, several of the large-scale analyses of knot invariants have been delegated to these repositories. This approach comes with both advantages and drawbacks, but the repositories are intended to remain dynamic and evolve over time, which motivated our choice. \diamond

The invariants we consider are the following (the homologies always categorify the associated polynomials). The reader unfamiliar with these can find more details in the references explaining the computation used. The data bases used are [LM25] for 3-16 crossings and [BBP25] for 17-18 crossings.

(a) Khovanov homology and odd Khovanov homology, both categorifying the Jones polynomial. We abbreviate these as K, O, and J, respectively.

(i) K was computed using the `KnotTheory` Mathematica package from [Atl24].

(ii) O was computed using the `KnotJob` program from [Sch25].

(iii) J was computed using a homemade program, that can be found on the page [KLTZ25].

For K and O we computed the homologies with rational coefficients, and their Poincaré polynomials are in $\mathbb{Z}_{\geq 0}[q, t]$ such that J is the specialization $t = -1$. We also consider the specialization $t = 1$ of K, called KT1. The data set is for 3-18 crossings.

(b) HFK homology and the Alexander polynomial, denoted HFK2 and A.

(i) HFK was computed using the Knot Floer homology calculator, [OS22], with algorithms from [OS19b] and [OS19a].

(ii) A was computed using the `KnotTheory` Mathematica package from [Atl24].

HFK was computed over \mathbb{F}_2 giving a polynomial in $\mathbb{Z}_{\geq 0}[q, t]$, and we also consider its $t = 1$ specialization with A being the $t = -1$ specialization. The data set is for 3-18 crossings.

(c) Khovanov–Rozansky homology for $n = 3$, categorifying the \mathfrak{sl}_3 polynomial. We denote them by KR3 (homology) and SL3 (polynomial).

(i) KR3 was computed using the `KnotJob` program from [Sch25].

(ii) SL3 was computed using the `KnotTheory` Mathematica package from [Atl24].

We used (and use below) the same conventions as for K. The data set for the homology is for 3-13 crossings, the polynomial for 3-18 crossings.

(d) HOMFLYPT homology and its decategorification the HOMFLYPT polynomial. These are denoted HH (homology) and H (polynomial).

(i) HH was computed with the program used in [NT21], available via the link in [NT21]. In contrast to the other invariants, this was computed using the knot data base in [Sto25] as it provides efficient braid presentations of the knots (which is very important for the used program). This is the bottle neck of the calculation: it ran for ≈ 215 days on the server of the Laboratoire de Mathématiques Blaise Pascal.

(ii) H was computed using the `KnotTheory` Mathematica package, [Atl24].

We used (and use below) the same conventions as for K. The data set for the homology is for 3-13 crossings, the polynomial for 3-16 crossings. Moreover, the data set is incomplete, as detailed in Table 5.

Remark 3.2. To the best of our knowledge, these homologies have not been computed on this scale before. \diamond

We are interested in how many distinct values these invariants take on the list of prime knots \mathcal{K}_n (with the same conventions as in [TZ25], e.g. not including mirrors and for $\leq n$ crossings), and we measure this as a percentage:

$$Q(n)_K^\% = \#\{Q(K) \mid K \in \mathcal{K}_n\} / \#\mathcal{K}_n.$$

These are the distinct values Q takes on prime knots (alternating and non-alternating).

The data is displayed in Figure 1 to Figure 4 and the precise values are listed in Table 2 to Table 5.

This motivates the analog of Theorem 2.18:

Corollary 3.3. (Exponential decay.) *For any polynomial or homological link invariant Q in Table 1 we have*

$$Q(n)_K^\% \in O(\delta^n) \text{ for some } \delta = \delta(Q) \in (0, 0.9993).$$

Moreover, Q detects knots with probability zero. \square

We anticipate that Corollary 3.3 extends to a wider range of link invariants and to links in place of knots, but we have no data to confirm this.

To conclude, we highlight the observations that we find the most surprising from our data:

- (a) The homologies perform only marginally better than the polynomials, and in fact, are essentially equivalent to two of their specializations. (HFK is a small exception.)
- (b) Odd Khovanov homology performs surprisingly poorly compared to standard Khovanov homology.
- (c) The SL3 polynomial detects nearly the same percentage of knots as the HOMFLYPT polynomial in our dataset.
- (d) HOMFLYPT homology is unexpectedly underwhelming: its detection rate does not seem to justify the computational cost. (The requirement of a braid presentation is a significant drawback; though this might improve if one could work directly from a PD presentation.)

REFERENCES

- [Ada94] C.C. Adams. *The knot book*. An elementary introduction to the mathematical theory of knots. W. H. Freeman and Company, New York, 1994.
- [AHT06] I. Agol, J. Hass, and W. Thurston. The computational complexity of knot genus and spanning area. *Trans. Amer. Math. Soc.*, 358(9):3821–3850, 2006. URL: <https://arxiv.org/abs/math/0205057>, doi:10.1090/S0002-9947-05-03919-X.
- [AFW15] M. Aschenbrenner, S. Friedl, and H. Wilton. Decision problems for 3-manifolds and their fundamental groups. In *Interactions between low-dimensional topology and mapping class groups*, volume 19 of *Geom. Topol. Monogr.*, pages 201–236. Geom. Topol. Publ., Coventry, 2015. URL: <https://arxiv.org/abs/1405.6274>, doi:10.2140/gtm.2015.19.201.
- [Atl24] K. Atlas. The Mathematica package *KnotTheory*‘, version September 27, 2024, 2024. URL: https://katlas.org/wiki/The_Mathematica_Package_KnotTheory%26gt;.
- [BN02] D. Bar-Natan. On Khovanov’s categorification of the Jones polynomial. *Algebr. Geom. Topol.*, 2:337–370, 2002. URL: <https://arxiv.org/abs/math/0201043>, doi:10.2140/agt.2002.2.337.
- [BN95] D. Bar-Natan. On the Vassiliev knot invariants. *Topology*, 34(2):423–472, 1995. doi:10.1016/0040-9383(95)93237-2.
- [Blo10] J.M. Bloom. Odd Khovanov homology is mutation invariant. *Math. Res. Lett.*, 17(1):1–10, 2010. URL: <https://arxiv.org/abs/0903.3746>, doi:10.4310/MRL.2010.v17.n1.a1.
- [BBP25] B.A. Burton, R. Budney, W. Pettersson and others. Regina: Software for low-dimensional topology. Version 2025. URL: <https://regina-normal.github.io>.
- [Cab13] S. Cabello. Hardness of approximation for crossing number. *Discrete Comput. Geom.*, 49(2):348–358, 2013. URL: <https://arxiv.org/abs/1204.0660>, doi:10.1007/s00454-012-9440-6.
- [Cha18] H. Chapman. On the structure and scarcity of alternating knots. 2018. URL: <https://arxiv.org/abs/1804.09780>.
- [DGS25] P. Dłotko, D. Gurnari, and R. Sazdanovic. Data driven perspectives on knot theory. 2025. URL: <https://arxiv.org/abs/2503.15103>.
- [DGS24] P. Dłotko, D. Gurnari, and R. Sazdanovic. Mapper–Type Algorithms for Complex Data and Relations. *J. Comput. Graph. Statist.*, 33(4):1383–1396, 2024. URL: <https://arxiv.org/abs/2109.00831>, doi:10.1080/10618600.2024.2343321.
- [FS09] P. Flajolet and R. Sedgewick. *Analytic combinatorics*. Cambridge University Press, Cambridge, 2009. doi:10.1017/CBO9780511801655.
- [GL89] C. McA. Gordon and J. Luecke. Knots are determined by their complements. *J. Amer. Math. Soc.*, 2(2):371–415, 1989. doi:10.2307/1990979.
- [Gre13] J.E. Greene. Lattices, graphs, and Conway mutation. *Invent. Math.*, 192(3):717–750, 2013. URL: <https://arxiv.org/abs/1103.0487>, doi:10.1007/s00222-012-0421-4.
- [Jae11] T.C. Jaeger. Khovanov–Rozansky homology and Conway mutation. 2011. URL: <https://arxiv.org/abs/1101.3302>.
- [Jon85] V.F.R. Jones. A polynomial invariant for knots via von Neumann algebras. *Bull. Amer. Math. Soc. (N.S.)*, 12(1):103–111, 1985. doi:10.1090/S0273-0979-1985-15304-2.
- [KLTVZ25] T. Kelomäki, A. Lacabanne, D. Tubbenhauer, P. Vaz, and V. Zhang. Code and more for the paper “On detection probabilities of link invariants”. 2025. <https://github.com/dtubbenhauer/knotdetection>, <https://dustbringer.github.io/web-knot-invariant-comparison/>.
- [Kho00] M. Khovanov. A categorification of the Jones polynomial. *Duke Math. J.*, 101(3):359–426, 2000. URL: <https://arxiv.org/abs/math/9908171>, doi:10.1215/S0012-7094-00-10131-7.
- [Kho02] M. Khovanov. A functor-valued invariant of tangles. *Algebr. Geom. Topol.*, 2:665–741, 2002. URL: <https://arxiv.org/abs/math/0103190>, doi:10.2140/agt.2002.2.665.
- [Kho06] M. Khovanov. Link homology and categorification. In *International Congress of Mathematicians. Vol. II*, pages 989–999. Eur. Math. Soc., Zürich, 2006.
- [KM11] P.B. Kronheimer and T.S. Mrowka. Khovanov homology is an unknot-detector. *Publ. Math. Inst. Hautes Études Sci.*, (113):97–208, 2011. URL: <https://arxiv.org/abs/1005.4346>, doi:10.1007/s10240-010-0030-y.
- [LTV24] A. Lacabanne, D. Tubbenhauer, and P. Vaz. Big data approach to Kazhdan–Lusztig polynomials. 2024. To appear in Journal of Experimental Mathematics. URL: <https://arxiv.org/abs/2412.01283>.
- [LC19] P. Lambert-Cole. On Conway mutation and link homology. *Adv. Math.*, 354:106734, 51, 2019. URL: <https://arxiv.org/abs/1701.00880>, doi:10.1016/j.aim.2019.106734.
- [Lee05] E.S. Lee. An endomorphism of the Khovanov invariant. *Adv. Math.*, 197 (2005), no. 2, 554–586. URL: <https://arxiv.org/abs/math/0210213>, doi:10.1016/j.aim.2004.10.015.
- [LHS22] J.S.F. Levitt, M. Hajij, and R. Sazdanovic. Big data approaches to knot theory: understanding the structure of the Jones polynomial. *J. Knot Theory Ramifications*, 31(13):Paper No. 2250095, 20, 2022. URL: <https://arxiv.org/abs/1912.10086>, doi:10.1142/s021821652250095x.
- [LM25] C. Livingston and A.H. Moore. Knotinfo: Table of knot invariants. URL: knotinfo.math.indiana.edu, 2025.

[MO08] C. Manolescu and P. Ozsváth. On the Khovanov and knot Floer homologies of quasi-alternating links. *J. Proceedings of Gökova Geometry-Topology Conference 2007*, 60–81. Gökova Geometry/Topology Conference (GGT), Gökova, 2008. URL: <https://arxiv.org/abs/0708.3249>.

[MC96] H.R. Morton and P.R. Cromwell. Distinguishing mutants by knot polynomials. *J. Knot Theory Ramifications*, 5(2):225–238, 1996. doi:10.1142/S0218216596000163.

[Mor15] H.R. Morton. Mutant knots. In *New ideas in low dimensional topology*, volume 56 of *Ser. Knots Everything*, pages 379–412. World Sci. Publ., Hackensack, NJ, 2015. doi:10.1142/9789814630627_0010.

[NT21] K. Nakagane and T. Sano. Computations of HOMFLY homology. 2021. To appear in *J. Knot Theory Ramifications*. URL: <https://arxiv.org/abs/2111.00388>, doi:10.1142/S0218216525500622.

[Oht02] T. Ohtsuki. *Quantum invariants*, volume 29 of *Series on Knots and Everything*. A study of knots, 3-manifolds, and their sets. World Scientific Publishing Co., Inc., River Edge, NJ, 2002.

[OS19a] P. Ozsváth and Z. Szabó. Algebras with matchings and knot Floer homology. 2019. URL: <https://arxiv.org/abs/1912.01657>.

[OS19b] P. Ozsváth and Z. Szabó. Bordered knot algebras with matchings. *Quantum Topol.*, 10(3):481–592, 2019. URL: <https://arxiv.org/abs/1707.00597>, doi:10.4171/QT/127.

[OS22] P. Ozsváth and Z. Szabó. Knot Floer homology calculator, version 3, July 13, 2022, 2022. URL: <https://web.math.princeton.edu/~szabo/HFKcalc.html>.

[Put16] K.K. Putyra. On a triply graded Khovanov homology. *J. Knot Theory Ramifications*, 25(3):1640011, 25, 2016. URL: <https://arxiv.org/abs/1501.05293>, doi:10.1142/S0218216516400113.

[RT91] N. Reshetikhin and V.G. Turaev. Invariants of 3-manifolds via link polynomials and quantum groups. *Invent. Math.*, 103(3):547–597, 1991. doi:10.1007/BF01239527.

[Sch25] D. Schütz. KnotJob, version August 15, 2025, 2025. URL: <https://www.maths.dur.ac.uk/users/dirk.schuetz/knotjob.html>.

[Shu21] A. Shumakovitch. Torsion in Khovanov homology of homologically thin knots. *J. Knot Theory Ramifications*, 30 (2021), no. 14, Paper No. 2141015, 17 pp. URL: <https://arxiv.org/abs/1806.05168>, doi:10.1142/S0218216521410157.

[ST98] C. Sundberg and M. Thistlethwaite. The rate of growth of the number of prime alternating links and tangles. *Pacific J. Math.*, 182(2):329–358, 1998. doi:10.2140/pjm.1998.182.329.

[Sto25] A. Stoimenow. Knot data tables, braid representatives and braid index, version 01.07.2025, 2025. URL: <https://stoimenov.net/stoimenov/homepage/ptab/>.

[Sto04] A. Stoimenow. On the number of links and link polynomials. *Q. J. Math.*, 55(1):87–98, 2004. doi:10.1093/qjmath/55.1.87.

[Tub25] D. Tubbenhauer. Quantum topology without topology. 2025. URL: <https://arxiv.org/abs/2307.00785>.

[TVW17] D. Tubbenhauer, P. Vaz, and P. Wedrich. Super q -Howe duality and web categories. *Algebr. Geom. Topol.*, 17(6):3703–3749, 2017. URL: <https://arxiv.org/abs/1504.05069>, doi:10.2140/agt.2017.17.3703.

[TZ25] D. Tubbenhauer and V. Zhang. Big data comparison of quantum invariants. 2025. To appear in *Journal of Experimental Mathematics*. URL: <https://arxiv.org/abs/2503.15810>.

[Tur94] V.G. Turaev. *Quantum invariants of knots and 3-manifolds*, volume 18 of *De Gruyter Studies in Mathematics*. Walter de Gruyter & Co., Berlin, 1994.

[Tut63] W.T. Tutte. A census of planar maps. *Canadian J. Math.*, 15:249–271, 1963. doi:10.4153/CJM-1963-029-x.

[Weh03] S.M. Wehrli. Khovanov homology and Conway mutation. 2003. URL: <https://arxiv.org/abs/math/0301312>.

[Weh10] S.M. Wehrli. Mutation invariance of Khovanov homology over \mathbb{F}_2 . *Quantum Topol.*, 1(2):111–128, 2010. URL: <https://arxiv.org/abs/0904.3401>, doi:10.4171/QT/3.

T.K.: AALTO UNIVERSITY, DEPARTMENT OF MATHEMATICS AND SYSTEMS ANALYSIS, OTAKAARI 1, 02150, ESPOO, FINLAND, ORCID 0000-0001-9714-3988
Email address: tuomas.kelomaki@aalto.fi

A.L.: LABORATOIRE DE MATHÉMATIQUES BLAISE PASCAL (UMR 6620), UNIVERSITÉ CLERMONT AUVERGNE, CAMPUS UNIVERSITAIRE DES CÉZEAX, 3 PLACE VASARELY, 63178 AUBIÈRE CEDEX, FRANCE, www.normalesup.org/~lacabanne, ORCID 0000-0001-8691-3270
Email address: abel.lacabanne@uca.fr

D.T.: THE UNIVERSITY OF SYDNEY, SCHOOL OF MATHEMATICS AND STATISTICS F07, OFFICE CARS LAW 827, NSW 2006, AUSTRALIA, www.dtubbenhauer.com, ORCID 0000-0001-7265-5047
Email address: daniel.tubbenhauer@sydney.edu.au

P.V.: INSTITUT DE RECHERCHE EN MATHÉMATIQUE ET PHYSIQUE, UNIVERSITÉ CATHOLIQUE DE LOUVAIN, CHEMIN DU CYCLOTRON 2, 1348 LOUVAIN-LA-NEUVE, BELGIUM, <https://perso.uclouvain.be/pedro.vaz>, ORCID 0000-0001-9422-4707
Email address: pedro.vaz@uclouvain.be

V.L.Z.: UNIVERSITY OF NEW SOUTH WALES (UNSW), SCHOOL OF MATHEMATICS AND STATISTICS, NSW 2052, AUSTRALIA, dustbringer.github.io, ORCID 0009-0007-5799-6477
Email address: victor.l.zhang@unsw.edu.au

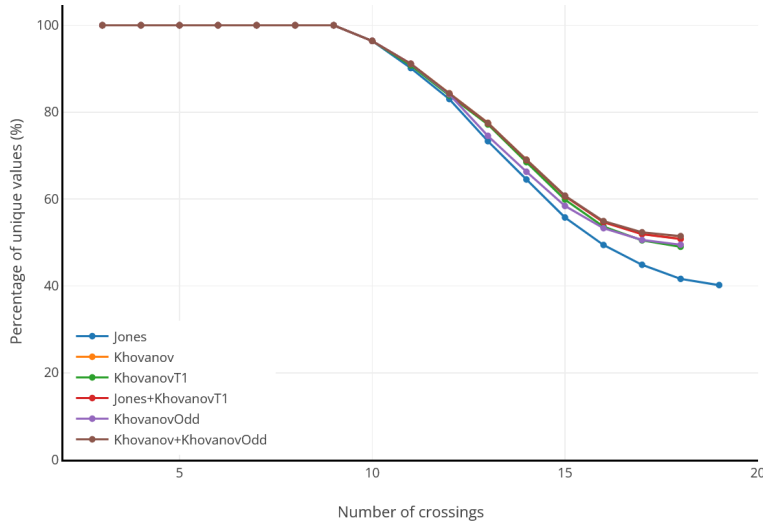


FIGURE 1. Percentage of unique values for the Jones family.

n	J	K	KT1	J+KT1	O	K+O
3	100.0	100.0	100.0	100.0	100.0	100.0
4	100.0	100.0	100.0	100.0	100.0	100.0
5	100.0	100.0	100.0	100.0	100.0	100.0
6	100.0	100.0	100.0	100.0	100.0	100.0
7	100.0	100.0	100.0	100.0	100.0	100.0
8	100.0	100.0	100.0	100.0	100.0	100.0
9	100.0	100.0	100.0	100.0	100.0	100.0
10	96.38	96.38	96.38	96.38	96.38	96.38
11	90.13	91.13	90.76	91.13	91.13	91.13
12	83.00	84.31	83.84	84.17	84.11	84.31
13	73.31	77.50	77.16	77.44	74.53	77.50
14	64.49	69.04	68.47	68.97	66.28	69.05
15	55.74	60.69	59.85	60.64	58.40	60.77
16	49.42	54.71	53.63	54.67	53.27	54.90
17	44.84	51.93	50.47	51.90	50.57	52.33
18	41.61	50.83	49.00	50.80	49.48	51.45
19	40.17	-	-	-	-	-

TABLE 2. Percentages of unique values for the Jones family; copyable data.

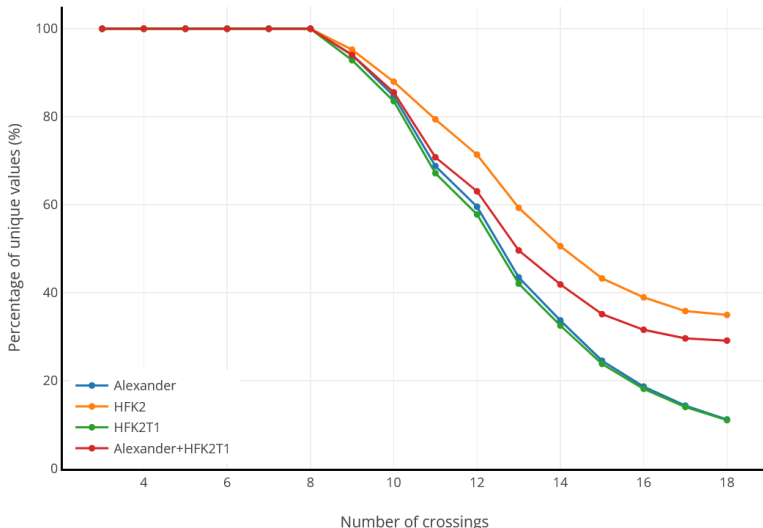


FIGURE 2. Percentage of unique values for the Alexander family.

n	A	HFK	HFKT1	A+HFKT1
3	100.0	100.0	100.0	100.0
4	100.0	100.0	100.0	100.0
5	100.0	100.0	100.0	100.0
6	100.0	100.0	100.0	100.0
7	100.0	100.0	100.0	100.0
8	100.0	100.0	100.0	100.0
9	94.04	95.23	92.85	94.04
10	84.73	87.95	83.53	85.54
11	68.78	79.40	67.16	70.78
12	59.55	71.38	57.8	63.05
13	43.49	59.31	42.08	49.61
14	33.69	50.57	32.54	41.89
15	24.55	43.27	23.82	35.13
16	18.65	38.96	18.15	31.57
17	14.35	35.82	14.04	29.61
18	11.19	34.95	11.05	29.11

TABLE 3. Percentages of unique values for the Alexander family; copyable data.

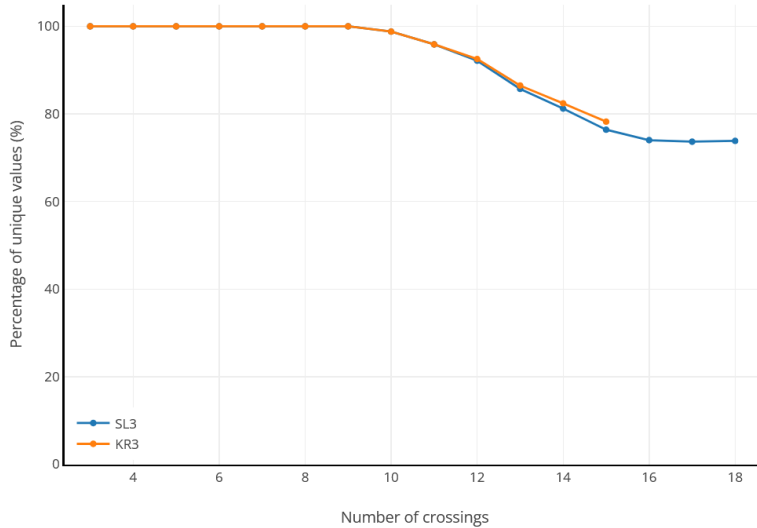


FIGURE 3. Percentage of unique values for the SL3 family. The comparison of specializations is not illustrated as the homology is essentially its Euler characteristic polynomial on the data set.

n	SL3	KR3
3	100.0	100.0
4	100.0	100.0
5	100.0	100.0
6	100.0	100.0
7	100.0	100.0
8	100.0	100.0
9	100.0	100.0
10	98.79	98.79
11	95.88	95.88
12	92.13	92.54
13	85.71	86.45
14	81.20	82.41
15	76.40	78.24
16	74.00	-
17	73.65	-
18	73.84	-

TABLE 4. Percentages of unique values for the SL3 family; copyable data.

Warning: The HOMFLYPT homology calculations for 12 and 13 crossings below are incomplete. The displayed data assumes all missing data give unique homologies, which places an upper bound on the values.

There are 219/2176 ($\approx 10.06\%$) and 3638/9988 ($\approx 36.42\%$) missing, for 12 and 13 crossings respectively. In both cases, knots with braid length ≥ 16 are missing and a few knots with shorter braid length did not finish.

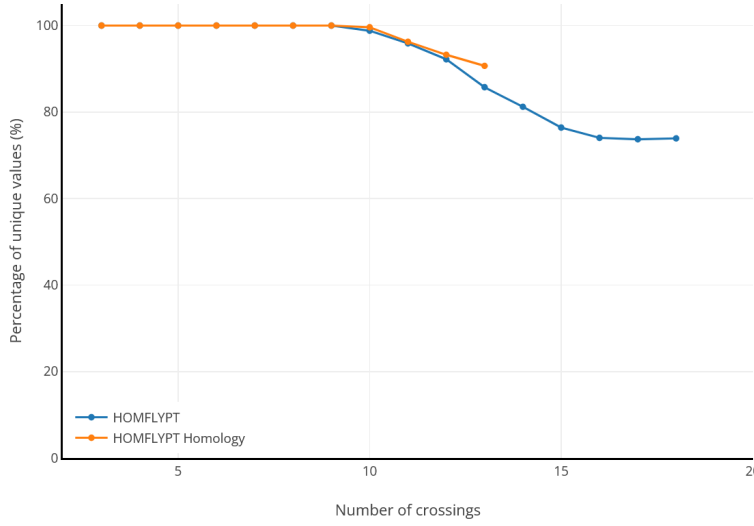


FIGURE 4. Percentage of unique values for the HOMFLYPT family. The comparison of specializations is not illustrated for the same reason as in [Figure 3](#).

n	H	HH
3	100.0	100.0
4	100.0	100.0
5	100.0	100.0
6	100.0	100.0
7	100.0	100.0
8	100.0	100.0
9	100.0	100.0
10	98.79	99.59
11	95.88	96.25
12	92.20	≤ 93.24
13	85.73	≤ 90.67
14	81.21	-
15	76.40	-
16	74.02	-
17	73.70	-
18	73.91	-

TABLE 5. Percentages of unique values for the HOMFLYPT family; copyable data.